Available online at www.sciencedirect.com

ScienceDirect

Advances in Space Research 68 (2021) 1975–1988

ADVANCES IN SPACE RESEARCH (a COSPAR publication)

www.elsevier.com/locate/asr

Thermal control of a spacecraft: Backward-implicit scheme programming and coating materials analysis

Vicent Alcayde [a], Ana Vercher-Martínez [a,b,*], F. Javier Fuenmayor [a,b]

[a] Depto. de Ingeniería Mecánica y de Materiales, Universitat Politècnica de València, Building 5E, Camino de Vera, 46022 Valencia, Spain
[b] Instituto de Ingeniería Mecánica y Biomecánica de Valencia - I2MB, Universitat Politècnica de València, Building 5E-9C, Camino de Vera, 46022 Valencia, Spain

Received 2 November 2020; received in revised form 15 March 2021; accepted 31 March 2021
Available online 14 April 2021

Abstract

The passive thermal control of a satellite consists of establishing the necessary thermal parameters involved in the process of heat transfer by radiation and conduction in order to delimit the range of temperatures to which the different components will be exposed. If the obtained range implies temperatures that the elements of the satellite are unable to cope with, therefore, an external control is demanded. This work deals with the programming of the equilibrium thermal problem taken into consideration a backward-implicit scheme. The algebraic mathematical approach for steady-state and transient analysis are implemented in Matlab© scripts. In addition, the work analyzes the influence of different coating materials on the passive thermal control of a benchmark spacecraft reported in the literature. The problem under scope considers the characteristics of a low Earth Orbit: the solar, albedo and planetary radiation, the radiation coming from other isotherm surfaces of the same satellite, the heat conduction and, finally, the radiation of these isotherm surfaces to the outer space. The procedure implemented is based on a feasible matrix formulation and results avoid the numerical instabilities prevalent in the forward-explicit approach, moreover, it enables further parametric and sensitivity analysis. Regarding the coating materials influence on the thermal response, the most relevant results evidence that thermal surfaces can guarantee the desirable range of temperature in a spacecraft. We confirm that certain material properties like the absorptance, emittance and its relation (absorption coefficient) are essential in the thermal response of the system. Nevertheless, these thermal properties do not influence in the same way. It is shown that the effect of the emittance is lower than the absorptance.

Keywords: Passive thermal control; Thermal balance; Thermal radiation; Spacecraft thermal analysis; Spacecraft coating materials; Backward-implicit scheme

1. Introduction

In every space mission involving the launch of a satellite, almost every part and gadget of the satellite being launched must meet certain criteria or requirements related to thermal behavior. The two main reasons behind the concerns of thermal control are: firstly, electronic and mechanical devices usually operate efficiently and reliably within relatively narrow temperature ranges, and secondly, most materials used in the satellites have non-zero coefficients of thermal expansion and, therefore, any considerable change in the temperature implies some kind of thermal distortion. In addition, in other applications, as in design of pico and nano-satellites (Bonnici et al., 2019; Corpino et al., 2015), passive thermal systems such as controlling conduction and radiation heat transfer paths, are the uniquely feasible option to fulfill the thermal requirements.

* Corresponding author at: Depto. de Ingeniería Mecánica y de Materiales, Universitat Politècnica de València, Building 5E, Camino de Vera, 46022 Valencia, Spain.
E-mail address: anvermar@dimm.upv.es (A. Vercher-Martínez).

https://doi.org/10.1016/j.asr.2021.03.041
0273-1177/

Nomenclature

P:	Power output of the Sun (estimated 384,6 yotta Watts)
d:	Distance from the Sun (m)
J_s:	Solar radiation at a given distance (W/m^2)
J_a:	Intensity of the albedo radiation (W/m^2)
J_p:	Earth's planetary radiation (W/m^2)
F:	Visibility factor
a:	Albedo parameter
R_{orbit}:	Distance between satellite and the center of the Earth (m)
R_{rad}:	Radius of the Earth's effective radiating surface (m)
α:	Absorptance of the material
ϵ:	Emitance of the material
A_{solar}:	Area receiving solar radiation (m^2)
A_{albedo}:	Area receiving albedo radiation (m^2)
$A_{planetary}$:	Area receiving planetary radiation (m^2)
A_{space}:	Total area of the satellite (m^2)
m_i:	Mass of each isothermal surface (kg)
C_i:	Specific heat (J/kg K)
ϵ_{ij}:	Effective emittance between two surfaces inside the satellite
h:	conductance (W/K)
A_iF_{ij}:	Product of area and radiation view factor
T_i:	nodal temperature (K)
σ:	Stefan–Boltzmann constant (5.669×10^{-8} W/m^2 K^4)
$Q_{internal}$:	Internal dissipated power (W)

In these cases, studying and developing new coating materials show a high interest because of the prominent influence that they exhibit on the system thermal behavior (Zhang et al., 2011).

The thermal requirements of a satellite mainly depend on the operating range of temperatures of its equipment or components. Usually, the temperature should be remain between −15 °C and 50 °C for the electronics, between 0 °C and 20 °C for rechargeable batteries, and around 0 °C and 50 °C for mechanisms such as gyroscopes, momentum wheels, solar array drives, etc. There are some exceptions, like in the case of some detectors found within astronomical telescopes, which need to be cooled down to very low temperatures, for instance. These temperature ranges can vary with the satellite characteristics (Bonnici et al., 2019; Corpino et al., 2015).

The environment to which the satellite is subjected is quite unique and distinctive. The high vacuum has some problems for the device while it takes away some others. Firstly, some satellites are placed into orbits where the residual atmospheric pressure (and, hence, drag) does, in order for them to maintain the orbit, force the satellite to re-boost itself, as the International Space Station (ISS) does. In the end, even though there is a light drag, it does not imply any friction, and thus, any heat. So, for this reason, convective interaction between spacecraft and environment will be ignored. Otherwise, there would be immense calculations referring to this heat, since it always varies depending on how low it is in the Earth's atmosphere. Generally, satellites orbit the Earth at around 300 km or more away from it. It can be measured that, in those altitudes, the atmospheric pressure drops to less than 10^{-7} mbar. Although there are some many more orbits with even less pressure, for sake of clarity, we are going to focus on this one. In Garzón and Villanueva, 2018 a detailed analysis of the single node model of a CubeSat is presented, varying the orbital position orientation the satellite orbital plane rotation and solar motion to the ecliptic.

A spacecraft mainly interacts with its environment by radiation, which is defined as the transmission of energy coming from different sources that will be considered at the current work (see Fig. 1).

Some codes have been developed over the years to perform thermal analysis in spacecraft. The one most commonly used in Europe is the ESA-sponsored ESATAN package and a spreadsheet-based program is also available in THERMXL (Knight et al., 2000).

In this work, the physical thermal problem is described in Section 2, summarizing the solar, albedo, planetary and spacecraft radiation (more details can be found in Fortescue et al. (2011)). In Section 3 a thermal analysis of an equatorial Low Earth Orbit satellite is presented followed by the lumped parameter model approach. The description of the materials considered in this work is detailed in Section 4. Subsequently, in Section 5 the backward-implicit scheme for the steady-state and transient regime is derived resulting in a matrix formulation. The Matlab© programming is also detailed. In Section 6, considering a benchmark satellite, the time history of the nodal temperature when different materials are used, denotes a high influence of the coating material in the passive thermal control. Finally, in Section 7 we summarize the work and the limitations.

2. Physical description of the thermal problem

2.1. Solar, Albedo and Planetary radiation

Solar radiation

Solar radiation is normally defined as the energy emitted by the sun. The solar radiation intensity will be calculated following the equation:

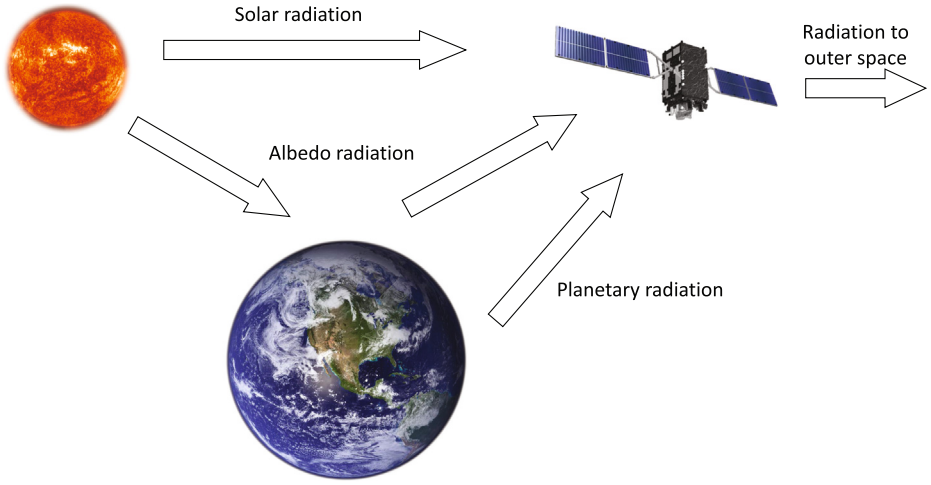

Fig. 1. Spacecraft thermal environment.

$$J_s = \frac{P}{4\pi d^2} \tag{1}$$

where P is defined as the power output of the Sun, being equal to 384,6 yotta Watts ($3{,}846\times10^{26}$ Watts) [4] and d being equal to the distance from the Sun.

Albedo

The albedo radiation is the measure of diffuse reflection of solar radiation out received from the Earth, in other words, it is the fraction of the solar radiation that is reflected from the surface of a planet. It is measured in a scale comprising between 0, which corresponds to a theoretical black body, and 1, to a body that reflects all incident radiation. The measurement of the albedo depends on several factors, such as the weather.

In order to calculate the intensity of the albedo radiation, J_a impinging on a spacecraft, it will be considered the following equation:

$$J_a = J_s aF \tag{2}$$

Being J_s the solar radiation at a given distance (see Eq. 1), a is the albedo parameter, in this work,we will take 0.33 as the Earth's albedo number, and F is the so-called visibility factor that varies with the altitude and the angle between the orbit plane and the Earth–Sun vector.

It is important to mention that for complex satellites, a more accurate calculus of the albedo radiation would be needed, that considers the orbital position for each external surface of the satellite (Bonnici et al., 2019).

Planetary radiation

Planetary radiation is the term we use to refer to the energy radiated from nearby planets. Although all planets in the solar systems have non-zero temperatures and consequently radiate heat, we will consider the Earth's planetary radiation as the main radiation from a planet affecting our analyzed spacecraft.

We define the planetary intensity with the following equation:

$$J_p = 237\left(\frac{R_{rad}}{R_{orbit}}\right)^2 \tag{3}$$

In Eq. 3, R_{orbit} is the distance to which the satellite is located from the center of the Earth, R_{rad} is the radius of the Earth's effective radiating surface. At the current work, the last term will be assumed to be equal to the Earth's surface radius. It is remarkable that such assumption would not be feasible for planets that lack an atmosphere and, therefore, have temperatures that vary way more than in the relatively controlled environment. The leading constant in the Eq. 3 is only valid for Earth.

2.2. Spacecraft radiation

Spacecraft radiation could be defined as the energy radiated from the spacecraft onto the deep space. This is the only radiation that does not belong to the boundary conditions, but it is necessary for describing the thermal equilibrium of the satellite at each time. The spacecraft radiation must be include in order to guarantee the thermal balance. Theoretically, the spacecraft has a finite temperature produced by the batteries, which are the only elements in the spacecraft which generate their own heat, and therefore radiating heat onto the environment. Moreover, in a assumed isolated environment, due to the heat of the batteries and the consequent radiation emitted from them, the environment would reach the same temperature as the batteries.

3. Thermal analysis

3.1. Introduction

As it has briefly mentioned in the last sections, temperature at each time must be in the operating temperature range according to the specific component. Thermal equilibrium has to be satisfied considering all heat sources and the different heat transfer mechanisms involved.

Therefore, clarifying when and how the external radiation will affect, it is necessary to assume that, firstly, the planetary radiation is independent of the position of the satellite, since it will always be at the same distance from the Earth, and this radiation cannot be blocked by anything. Secondly, the solar radiation is dependent on the position of the satellite and the possibility of being blocked from the Sun by the Earth. In order to simplify the calculations a bit, we will suppose the satellite orbits the Earth following its equator. Thus, the satellite will receive solar radiation when it is situated on the sunlit trace of its orbit. Finally, since the albedo radiation depends on the solar radiation, it will radiate the satellite whenever the sun does. It is a complicated and varying number, that, as we have stated before, is simplified in an average.

To sum up, there are two situations in which the satellite is under the effect of the sum of different values, both of them explained in more detailed in the next sections (see Fig. 2):

- Sunlight zone: Radiation received = Solar rad + Albedo rad + Planetary rad
- Shadow zone: Radiation received = Planetary rad

Hence, knowing all the main radiations loads that the spacecraft receives during its lifetime orbiting the Earth and the time periods during which it experiences those loads, it is necessary to determine if it would be necessary to use equipment for active thermal control, gadgets and mechanisms that require a certain range of temperatures in the case of the satellite not being able to dissipate all the heat by itself or not being able to cope temperatures that are too low.

3.2. Thermal balance

It has already been mentioned that to maintain an adequate temperature for a satellite's mechanisms and gadgets proper functioning depends directly on the balance between the heat received from all the aforementioned external radiations, the internal heat and the heat radiated from the spacecraft to the environment. This correlation, from which we obtain the equilibrium temperature, is explained by the following equation:

$$\alpha A_{solar} J_s + \alpha A_{albedo} J_a + \epsilon A_{planetary} J_p + Q_{internal} = \epsilon \alpha A_{space} T^4 \quad (4)$$

Every component of the Eq. 4 equals to one of the aforementioned parts that alter the balance and equilibrium of temperatures, being:

- Solar radiation: $\alpha A_{solar} J_s$
- Albedo radiation: $\alpha A_{albedo} J_a$
- Planetary radiation: $\epsilon A_{planetary} J_p$
- Internal dissipated power: $Q_{internal}$
- Heat radiated to space: $\epsilon \alpha A_{space} T^4$

Through Eqs. (1)–(3), the terms J_a, J_p and J_s can be obtained:

$$J_p = 220 \text{ W/m}^2$$
$$J_s = 1371 \text{ W/m}^2$$
$$J_a = 0.33 F J_s \text{ W/m}^2 \text{ (Earth albedo a = 0.33)}$$

where J_p corresponds to an orbit altitude of 240 km and J_a corresponds to a visibility factor $F = 0.15$ for 100 % sunlit orbit and $F \approx 0.7$ for the sunlit in a cold orbit.

In addition, the variables α and ϵ are the absorptance and emittance of the surface's material, respectively. These will be the parameters that will undergo modifications in the following sections in order to analyze different materials, their effectiveness and behavior, and how they shield from the different radiations.

Finally, A_{solar}, A_{albedo} and $A_{planetary}$ are the areas receiving, respectively, solar, albedo and planetary radiation; on a side note, A_{space} is the total area of the satellite.

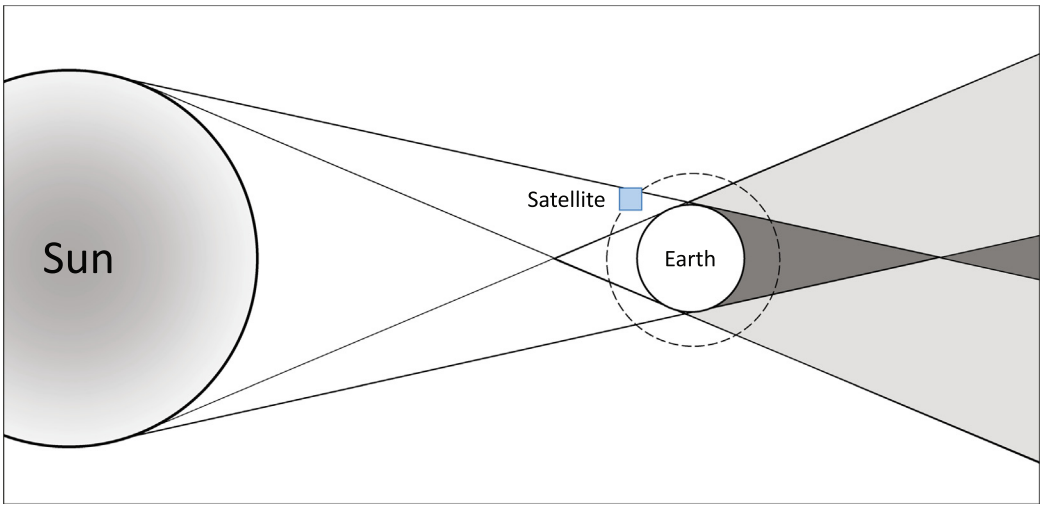

Fig. 2. Schematic representation of different stages of the satellite in its trajectory.

3.3. Lumped parameter model. Nodal analysis

The lumped parameter model consists in representing the isotherm surfaces in a reduced number of nodes. The following equation represents the relationship between all radiations affecting the satellite, the internal heat, the radiation that the satellite itself radiates to the space, and the division and characteristics of each node (Fortescue et al., 2011):

$$m_i C_i \frac{dT_i}{dt} = Q_{external,i} + Q_i - \sigma \epsilon_i A_{space,i} T_i^4 - \sum_{j=1}^{n} h_{ij}(T_i - T_j) - \sigma \sum_{j=1}^{n} A_i F_{ij} \epsilon_{ij} (T_i^4 - T_j^4) \quad (5)$$

In Eq. 5, m_i equates to the mass of each isotherm surface, c_i is the specific heat of each node, which would depend on the material used to build the satellite, and not on the coat or material used on the surface.

Being $Q_{external}$ calculated by means of the following equation:

$$Q_{external,i} = J_s \alpha_i A_{solar,i} + J_a \alpha_i A_{albedo,i} + J_p \epsilon_i A_{planetary,i} \quad (6)$$

In Eq. 5, ϵ_{ij} is the effective emittance between two surfaces inside the satellite. It has a complicated dependence on surfaces' optical properties, mutual reflections and reflections via other nearby surfaces. Owing to the fact that errors from this value are rather small, and that the surfaces involved are diffuse and have a relatively high ϵ value, it is okay to assume that the interior all of them is painted in white, and that their emittance values are equal to 0,82.

Finally, the term h is the conductance and the product $A_i F_{ij}$ represents the *area* × *view factor*.

3.3.1. Steady state

The steady-state case consists on calculating the temperatures of each node of the satellite in a certain moment. When the steady-state is analyzed, it is done by assuming it in the sunlight zone in order to calculate the worst case scenario, that is to say, one in which $Q_{external}$ will be constant and equal to the sum of all the radiations introduced previously.

Following Fortescue et al. (2011), Eq. 5 will be linearized:

If $T_{i,0}$ represents the temperature of the ith node at time t_0, the temperature of that node in a forward δt is given by:

$$T_i = T_{i,0} + \delta T_{i,0} \quad \text{where} \quad \delta T_{i,0} = \frac{dT_{i,0}}{dt} \delta t \quad (7)$$

Assuming $\delta T_{i,0}$ is small compared with $T_{i,0}$, we have:

$$T_i^4 = (T_{i,0} + \delta T_{i,0})^4 \approx T_{i,0}^4 + 4 T_{i,0}^4 \delta T_{i,0} \quad (8)$$

Therefore,

$$T_i^4 \approx T_i(4 T_{i,0}^3) - 3 T_{i,0}^4 \approx T_{i,0}^4 + 4 T_{i,0}^4 \delta T_{i,0} \quad (9)$$

By substituting this linearization in the nodal analysis' main equation and considering $\frac{dT_i}{dt} = 0$, the following equation is derived:

$$T_i \left[\sum_{j=1}^{n} h_{ij} + 4\sigma T_{i,0}^3 \left(A_{space,i} \epsilon_i + \sum_{j=1}^{n} A_i F_{ij} \epsilon_{ij} \right) \right] - \sum_{j=1}^{n} T_j \left[h_{ij} + 4\sigma T_{j,0}^3 A_i F_{ij} \epsilon_{ij} \right] = Q_{external,i} + Q_i + 3\sigma T_{i,0}^3 A_{space,i} \epsilon_i + 3\sigma \sum_{j=1}^{n} (T_{i,0}^4 - T_{j,0}^4) A_i F_{ij} \epsilon_{ij} \quad (10)$$

3.3.2. Transient

In the transient analysis, unlike with the steady-state, we analyze the satellite performance taking into consideration the time, the movement that it has and the temperatures' evolution. We take into account whether the satellite stands in either the sunlight or shadow zones, and the corresponding radiations that affect it at every moment. As well as with the steady-state nodal analysis, the transient nodal analysis needs the use of numerical methods and linearization in order to be calculated. In addition, we substitute the left member of the nodal analysis equation (Eq. 5) by the following expression:

$$m_i C_i \frac{dT_i}{dt} \rightarrow m_i C_i \frac{(T_i - T_{i,0})}{\delta t} \quad (11)$$

Furthermore, we will also substitute the temperature and heat inputs by the average values over the time interval δt:

$$\begin{aligned} T_i &\rightarrow (T_i + T_{i,0})/2 \\ T_j &\rightarrow (T_j + T_{j,0})/2 \\ Q_{external,i} &\rightarrow (Q_{external,i} + Q_{external,0})/2 \end{aligned} \quad (12)$$

By doing these substitutions, we provide the temperature history at successive intervals of time. The shorter the interval, the less the temperatures will vary, which will consequently provide us a more hopefully graph of each node's evolution of temperatures.

The general heat transfer equation can be discretised using the finite difference method and solved with a forward-explicit procedure (Chapman, 1987). For instance, in Bonnici et al. (2019), the problem is solved using this approach for a lumped mass model of a pico-satellite of 17 nodes. However, in order to avoid instabilities in the solution process, it is recommended to employ a backward-implicit scheme (Gilmore, 2002).

In this work, the lumped mass approximation is used to model the thermal behavior of a representative satellite, programming a backward-implicit procedure in Matlab©. The matrix formulation is also presented, which resolution requires to solve the numerical system of algebraic equations.

4. Materials

4.1. Introduction

Knowing the properties of the materials proves crucial when selecting one specific coating for the spacecraft's surface. The solar absorptance and thermal emittance of a material are two essential characteristics when determining the spacecraft's temperature control. Hence, a list with some of the most important and broadly used materials in aerospace engineering is shown in Table 1.

4.2. Structural materials

Firstly, defining the structural materials, or the materials that the satellite is mainly made of, is a very important decision and it will therefore have an impact on the calculations of our analysis. The structural materials are the

Table 1
Spacecrafts' coating materials (Kauder, 2005).

Material	Absorptance, α	Emittance, ϵ	Absortion coefficient, α/ϵ
	Optical solar reflectors		
Silvered fused silica	0,07	0,8	0,0875
Indium - Tin - Oxide (ITO)	0,07	0,76	0,0921
Aluminized Teflon (0,5 mm)	0,14	0,4	0,35
Aluminized Teflon (10 mm)	0,15	0,85	0,1765
Silvered Teflon (2 mm)	0,08	0,68	0,1176
Silvered Teflon (10 mm)	0,09	0,88	0,1023
	Black coatings		
Catalac black paint	0,96	0,88	1,091
Delrin black plastic	0,96	0,87	1,1034
Martin black velvet paint	0,91	0,94	0,9681
Parsons black paint	0,98	0,91	1,0769
Vel-black	0,99	0,95	1,0421
	White coatings		
Barium sulphate with polyvinyl alcohol	0,06	0,91	0,0659
Catalac white plastic	0,24	0,9	0,267
NASA/GSFC NS-74 White paint	0,17	0,92	0,267
Magnesium oxide aluminium oxide paint	0,09	0,92	0,0978
White polyurethane paint	0,27	0,84	0,3214
	Anodized aluminium samples		
Anodized aluminium black	0,76	0,88	0,8636
Anodized aluminium blue	0,60	0,88	0,6816
Anodized aluminium chromic	0,44	0,56	0,7857
Anodized aluminium gold	0,48	0,82	0,5854
Anodized aluminium red	0,57	0,88	0,6477
Anodized aluminium yellow	0,47	0,87	0,5402
	Film and tapes		
Aluminium tape	0,21	0,04	5,25
Aluminized aclar film (1 mm)	0,12	0,54	0,22
Aluminized kapton (aluminium outside)	0,14	0,05	2,8
Goldized kapton (gold outside)	0,25	0,02	12,5
	Metals		
Buffed aluminium	0,16	0,03	5,33
Buffed copper	0,30	0,03	10
Polished aluminium	0,24	0,08	3
Polished Beryllium	0,44	0,01	44
Polished Gold	0,30	0,05	6
Polished Silver	0,04	0,02	2
Polished Stainless steel	0,42	0,11	3,818
Polished Tungsten	0,44	0,03	14,67
	Vapor-deposited coatings		
Aluminium	0,08	0,02	4
Gold	0,19	0,02	9,5
Silver	0,04	0,02	2
Titanium	0,51	0,12	4,33
Tungsten	0,60	0,27	2,22
Polished Silver	0,04	0,02	2
	Solar cells		
Galium arsenide-based solar cells	0,88	0,80	1,1
Crystalline silicon-based solar cells	0,75	0,82	0,915

ones that will conduct the heat, and its specific heat, amongst other things, defines how easy will it be to increase the temperature. Based on the aforementioned, a low specific heat reduces the amount of energy required to increase the temperature of a unit mass of material by one unit of temperature. The material also defines, obviously, the weight of the satellite. The heavier a satellite, the worse, as the launch vehicle will have to lift more weight per satellite, thus being able to carry fewer satellites. Summing up, we require a structural material that meets a low specific heat and low density, so it does not weigh too much and transmits little heat. The most commonly used materials in the aerospace field are titanium, carbon fiber and aluminium.

4.3. Coating materials

The coating materials used on a satellite greatly influence how the satellite will do in terms of coping with heat loads, and in what measure they will influence the spacecraft. For this reason, based on the well-explained programming in the next section, we will summarize the materials analyzed. Each material will be described based on its thermal emittance, ϵ, and solar absorptance, α, essential factors, as it was said, for the calculation of the temperatures in function of which material is used on the satellite's surface (Fortescue et al., 2011,-Kauder (2005).

5. Matlab programming

5.1. Introduction

As it has been briefly stated previously in this work, Matlab, abbreviation of **Mat***rix* **Lab***oratory*, is a very powerful and competent calculation engine, able to offer an integrated development environment (IDE) with its own programming language (M language).

Thermal nodal balance has been programmed considering the steady-state regime, in which we just contemplate the satellite in the sunlight zone, being radiated by solar, albedo and planetary radiation, and the transient regime, where the nodal temperature evolution is calculated around the movement of the satellite in its orbit.

5.2. Steady state. Matrix formulation

One of the goals of the current work is to develop the matrix formulation of the system of equations given by Eq. 10 that governs the steady-state analysis. For sake of clarity, n nodes have been considered.

At the beginning, we must define all the constants that our problem needs, such as the *view factor* × *area*, the conductance, the areas of the nodes, their internal heat and the initial temperatures, among others.

$$\begin{bmatrix} \sum_{j=1}^{n} h_{1j} + 4\sigma T_{1,0}{}^{3}\left(A_{space,1}\epsilon_1 + \sum_{j=1}^{n} A_j F_{1j}\epsilon_{1j}\right) & -\left(h_{12} + 4\sigma T_{2,0}{}^{3} A_1 F_{12}\epsilon_{12}\right) & \cdots \\ -\left(h_{21} + 4\sigma T_{1,0}{}^{3} A_1 F_{21}\epsilon_{21}\right) & \sum_{j=1}^{n} h_{2j} + 4\sigma T_{2,0}{}^{3}\left(A_{space,2}\epsilon_2 + \sum_{j=1}^{n} A_j F_{2j}\epsilon_{2j}\right) & \cdots \\ \vdots & \vdots & \ddots \\ -\left(h_{n1} + 4\sigma T_{1,0}{}^{3} A_n F_{n1}\epsilon_{n1}\right) & -\left(h_{n2} + 4\sigma T_{2,0}{}^{3} A_n F_{n2}\epsilon_{n2}\right) & \cdots \end{bmatrix}$$

$$\begin{bmatrix} \cdots & -\left(h_{1n} + 4\sigma T_{n,0}{}^{3} A_1 F_{1n}\epsilon_{1n}\right) \\ \cdots & -\left(h_{2n} + 4\sigma T_{n,0}{}^{3} A_2 F_{2n}\epsilon_{2n}\right) \\ \ddots & \vdots \\ \cdots & \sum_{j=1}^{n} h_{nj} + 4\sigma T_{n,0}{}^{3}\left(A_{space,n}\epsilon_n + \sum_{j=1}^{n} A_j F_{njnj}\right) \end{bmatrix} \begin{pmatrix} T_1 \\ T_2 \\ \vdots \\ T_n \end{pmatrix} =$$

$$= \begin{pmatrix} Q_{external,1} + Q_1 + 3T_{1,0}{}^{4}\sigma A_{space,1}\epsilon_1 + 3\sigma\sum_{j=1}^{n} A_1 F_{1j}\epsilon_{1j}\left(T_{1,0}{}^{4} - T_{j,0}{}^{4}\right) \\ Q_{external,2} + Q_2 + 3T_{2,0}{}^{4}\sigma A_{space,2}\epsilon_2 + 3\sigma\sum_{j=1}^{n} A_2 F_{2j}\epsilon_{2j}\left(T_{2,0}{}^{4} - T_{j,0}{}^{4}\right) \\ \vdots \\ Q_{external,n} + Q_n + 3T_{n,0}{}^{4}\sigma A_{space,n}\epsilon_n + 3\sigma\sum_{j=1}^{n} A_n F_{nj}\epsilon_{nj}\left(T_{n,0}{}^{4} - T_{j,0}{}^{4}\right) \end{pmatrix} \tag{13}$$

In Matlab, the unknown term (nodal temperatures) is calculated as follows:

Temperatures = Matrix\Last;

where *Matrix* contain the coefficient terms:

M(i,i)=Sumj_(h_vector(i,j))+4*sigma*T_0_vector(i)^(3)*(A_space_vector(i)*epsilon_inside(i)+Sumj_(F_vector(i,j)*epsilon(i,j)));

And another term away from the main diagonal is given by:

M(i,j)=-(h_vector(i,j)+4*sigma*T_0_vector(j)^(3)*F_vector(i,j)*epsilon(i,j));

The next step is to develop the independent term *Last* of the matrix equation. It is done as follows, having as example the first component of this vector:

L(i)=Q_ext(i)+Q_vector(i)+3*sigma*T_0_vector(i)^(4)*A_space_vector(i)*epsilon_inside(i)+3*sigma*Sumj_((T_0_vector(i)^(4)-T_0_vector(j)^(4))*F_vector(i,j)*epsilon(i,j));

being $Q_{external}$:

Q_ext(i)=Js*alpha_outside*A_solar + Ja_sun*alpha_outside*A_albedo + Jp*epsilon_outside*A_planetary;

An iterative procedure is programmed to calculate the temperatures in which the satellite will stabilize. The temperatures calculated in a step are the initials for the next, updating *Matrix* and *Last* to the new temperature values. This iteration is done with the command function, calling the other scripts and feeding them the new values of initial temperatures. It is done as follows:

[Matrix]=Matrix_Components(epsilon_inside,sigma,F_vector,h_vector,epsilon,T_0_vector,A_space_vector);
[Last]=Last_Component(Q_ext,Q_vector,sigma,T_0_vector,A_space_vector,F_vector,epsilon_outside,epsilon_inside,epsilon);

5.3. Transient. Matrix formulation

First of all, in order to program the transient analysis, we need to think about all the situations that the satellite will go through. In the transient analysis, the orbit followed is a Low Earth Orbit (LEO) and a Near Equatorial Orbit, meaning that our satellite will orbit with an inclination near to zero taking the equatorial plane as a reference. Following a LEO orbit means that the satellite will complete geocentric orbits with an altitude of around 240 km, taking it approximately 1 h, 29' and 18" to do the whole orbit. In this work, we will suppose that the spacecraft will be 59 % out of the whole orbit exposed to the Sun and, consequently, receiving solar, albedo and planetary radiation during this time bracket. This situation would correspond with a cold case orbit, when the Earth–Sun vector lies in the plane of the orbit. During the remaining time, it will be behind the Earth, assuming that only receive planetary radiation. To sum up, the whole orbit is equal to 5,358 s, and the time it will be in the Sunlight zone will be around 3,161 seconds.

The matrix formulation of the governing equation Eq. 5 is derived in the current work:

$$\begin{bmatrix} \frac{m_1C_1}{2\Delta t}+\frac{\sigma\epsilon_1A_1{4T_{1,0}}^3}{2}+\sum_{j=1}^{n}\left(\frac{h_{1j}}{2}+\frac{\sigma A_1F_{1j}\epsilon_{1j}{4T_{1,0}}^3}{2}\right) & -\frac{h_{12}}{2}-\frac{\sigma A_1F_{12}\epsilon_{12}{4T_{2,0}}^3}{2} & \cdots \\ -\frac{h_{21}}{2}-\frac{\sigma A_2F_{21}\epsilon_{21}{4T_{1,0}}^3}{2} & \frac{m_2C_2}{2\Delta t}+\frac{\sigma\epsilon_2A_2{4T_{2,0}}^3}{2}+\sum_{j=1}^{n}\left(\frac{h_{2j}}{2}+\frac{\sigma A_2F_{2j}\epsilon_{2j}{4T_{2,0}}^3}{2}\right) & \cdots \\ \vdots & \vdots & \ddots \\ -\frac{h_{n1}}{2}-\frac{\sigma A_nF_{n1}\epsilon_{n1}{4T_{1,0}}^3}{2} & -\frac{h_{n2}}{2}-\frac{\sigma A_nF_{n2}\epsilon_{n2}{4T_{2,0}}^3}{2} & \cdots \end{bmatrix}$$

$$\begin{bmatrix} \cdots & -\frac{h_{1n}}{2}-\frac{\sigma A_1F_{1n}\epsilon_{1n}{4T_{n,0}}^3}{2} \\ \cdots & -\frac{h_{2n}}{2}-\frac{\sigma A_2F_{2n}\epsilon_{2n}{4T_{n,0}}^3}{2} \\ \ddots & \vdots \\ \cdots & \frac{m_nC_n}{2\Delta t}+\frac{\sigma\epsilon_nA_n{4T_{n,0}}^3}{2}+\sum_{j=1}^{n}\left(\frac{h_{nj}}{2}+\frac{\sigma A_nF_{nj}\epsilon_{nj}{4T_{n,0}}^3}{2}\right) \end{bmatrix}\begin{pmatrix} T_1 \\ T_2 \\ \vdots \\ T_n \end{pmatrix}=$$

$$=\begin{matrix} \frac{m_1C_1T_{1,0}}{2\Delta t}+\frac{Q_{ex,1}+Q_{ex,1,0}}{2}+Q_1-\frac{\sigma\epsilon_1A_{space,1}{4T_{1,0}}^3}{2}+\sigma\epsilon_1A_{space,1}{3T_{1,0}}^4- \\ \frac{m_2C_2T_{2,0}}{2\Delta t}+\frac{Q_{ex,2}+Q_{ex,2,0}}{2}+Q_2-\frac{\sigma\epsilon_2A_{space,2}{4T_{2,0}}^3}{2}+\sigma\epsilon_2A_{space,2}{3T_{2,0}}^4- \\ \vdots \\ \frac{m_nC_nT_{n,0}}{2\Delta t}+\frac{Q_{ex,n}+Q_{ex,n,0}}{2}+Q_n-\frac{\sigma\epsilon_nA_{space,n}{4T_{n,0}}^3}{2}+\sigma\epsilon_nA_{space,n}{3T_{n,0}}^4- \\ -\sum_{j=1}^{n}\left[\frac{h_{1j}T_{1,0}}{2}-\frac{h_{1j}T_{j,0}}{2}-\sigma\left(-\frac{A_1F_{1j}\epsilon_{1j}{4T_{1,0}}^3}{2}+A_1F_{1j}\epsilon_{1j}{3T_{1,0}}^4+\frac{A_1F_{1j}\epsilon_{1j}{4T_{j,0}}^3}{2}-A_1F_{1j}\epsilon_{1j}{3T_{j,0}}^4\right)\right] \\ -\sum_{j=1}^{n}\left[\frac{h_{2j}T_{2,0}}{2}-\frac{h_{2j}T_{j,0}}{2}-\sigma\left(-\frac{A_2F_{2j}\epsilon_{2j}{4T_{2,0}}^3}{2}+A_2F_{2j}\epsilon_{2j}{3T_{2,0}}^4+\frac{A_2F_{2j}\epsilon_{2j}{4T_{j,0}}^3}{2}-A_2F_{2j}\epsilon_{2j}{3T_{j,0}}^4\right)\right] \\ \vdots \\ -\sum_{j=1}^{n}\left[\frac{h_{nj}T_{n,0}}{n}-\frac{h_{nj}T_{j,0}}{2}-\sigma\left(-\frac{A_nF_{nj}\epsilon_{nj}{4T_{n,0}}^3}{2}+A_nF_{nj}\epsilon_{nj}{3T_{n,0}}^4+\frac{A_nF_{nj}\epsilon_{nj}{4T_{j,0}}^3}{2}-A_nF_{nj}\epsilon_{nj}{3T_{j,0}}^4\right)\right] \end{matrix} \quad (14)$$

As for the steady-state approach, in the above matrix equation, the counter j takes values from 1 to n, excluding the number corresponding to the equation i. For example, for the first equation, j takes values from 2 to n.

First and foremost, as we already did in the steady-state analysis, we need to define the constants that will be used thereupon. Exactly the same constants and variables in the steady-state programming will be defined in this case, in addition to some others such as the seconds that a lap lasts, the mass and the specific heat of each node, among many others. We will need to define some vectors assigning them the size we want them to have, in order to avoid problems with them changing size every time a loop operation is completed.

As mentioned above, the external radiation loads change depending on the satellite's position in orbit. Since we need to calculate the average value of the external radiation that the satellite is receiving at this moment in our programming, and the radiation that it was receiving in the moment before, we will discern between sunlight zone, shift, and shadow.

6. Results

This section shows the results for the thermal transient analysis problem considering different coating materials, throughout the backward-implicit scheme implemented. The steady-state results are usually considered as the initial temperatures for the transient analysis.

The results correspond to the complete analysis of temperatures in a whole orbit around the Earth. Several rounds will be shown in there in order to make clear the stabilization that the satellite sustains during its trajectory, beginning with an illustrative temperature. This stabilization consists on temperatures cycles, that reach maximum and minimum depending on where the satellite is. It is clearly distinguished between the zone in which the satellite receives solar, albedo and planetary radiation, which is the sunlight zone, and the zone where it only receives planetary radiation, which is the shadow zone.

The graphics represent the nodal temperature evolution for a particular material. The parameters that are modified are the absorptance and the emittance.

6.1. Numerical example

For the sake of simplicity, let's consider an air density measurement spherical spacecraft, 1 meter of diameter, was assumed, as shown in the Fig. 3 (Fortescue et al., 2011).

The spacecraft is spinning around the spin axis indicated in the Fig. 3 that will remain perpendicular to the solar radiation during the entire orbit. No control system of spinning has been modeled in this work.

In the analysed example, the only source of internal dissipation is at the centre, corresponding to the battery-beacon package. In this circumstance, we may assume that temperatures vary only with spacecraft 'latitude'. Each hemisphere has been divided in isothermal surfaces generated by cutting planes parallel to the satellite equator. In order to analyze the distribution of temperatures in the spacecraft, we will divide the external shield of the satellite into 6 parts with the same surface, as shown in the Fig. 3.

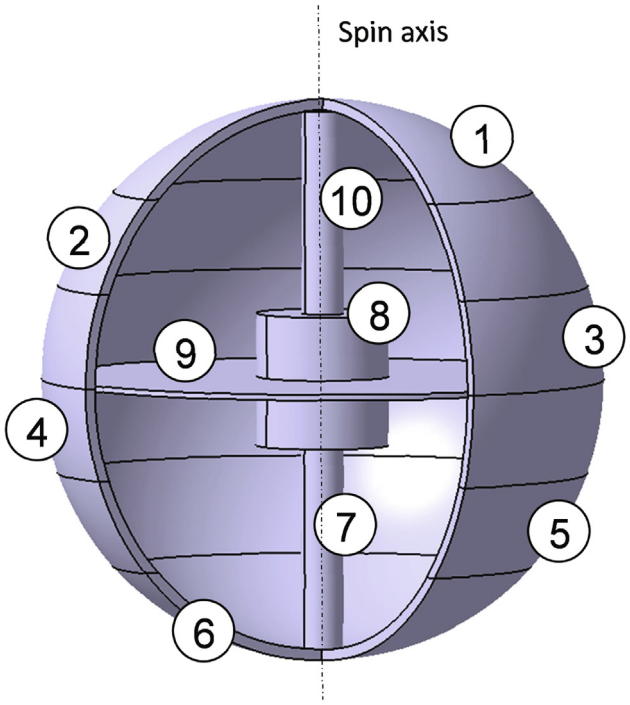

Fig. 3. Lumped model of the benchmark spacecraft analyzed in this work (Fortescue et al., 2011).

We will also divide the internal components, such as the superior and inferior axis (numbers 10 and 7, respectively), a central plate for support (number 9) and the batteries (number 8). The batteries are the only ones that produce internal heat. The initial temperature is assumed 293 K for the battery and 273 K for the rest of nodes. In addition, it is assumed that the satellite radiates heat into space as a black body, at 0 K.

We can assume and calculate the different areas, and, since A_{solar}, A_{albedo} and $A_{planetary}$ are the same, and equal to the area of a circle, this is what it is seen from one side of the satellite:

$$A_{solar},\ A_{albedo},\ A_{planetary} = \pi r^2 = \frac{\pi}{4}$$

$$A_{space} = 4\pi r^2 = \pi \tag{15}$$

All nodes in the surface (from 1 to 6) have the same thickness and area, consequently they will have the same mass; C_i is the specific heat of each node, which would depend on the material used to build the satellite.

The *area* × *view factor* relating 2 surfaces each time are summarized in Table 2. In addition, the conductance term, which depends on the shape, is also shown in the Table 3:

Besides the batteries, which made of Lithium-Ion, and the external coating, all the other parts will supposed to be made out of aluminium. Thus, in order to calculate its mass, we will make use of the following equations, with them depending ones on each node, since they have different shapes, and acknowledging that the density of the aluminium is equal to 2,7 g/cm^3: from m_1 to $m_6 = 27,16$kg, $m_7 = m_{10} = 5,24$ kg, $m_9 = 19,54$ kg (gold plate), $m_8 = 8,08$kg (batteries). Additionally, the specific heat (J/kg K) for aluminium is 880 and for Lithium-Ion batteries, 950.

6.2. Results for different coating materials

The programmed code in Matlab© has been run in order to obtain the numerical simulation of the thermal behavior of the benchmark spacecraft described in Section 6.1 considering different coating materials.

Taking into consideration the operating ranges of temperatures of each part of the satellite (between 0°C and 20°C for rechargeable batteries), we can observed that materials based on black coatings accomplishes with this specification (see Fig. 4).

In the following graphs, the nodal temperature evolution for transient analysis is shown for some representative coating materials that are selected from every family depicted in Table 1. In the abscissa's axis, the represented magnitudes are the time in second and the number of orbits (see Figs. 5–13).

Basing on the results shown, we can confirm that the absorptance and emittance of the materials determine the thermal response of the system. If we consider the results obtained for Vel-Black (see Fig. 4), we can discern pretty well the difference between the sunlight zone and the shadow zone, and how these changes affect the temperature of the spacecraft. Note that in the graphic it is displayed from the tenth to the fourteenth orbit, in order to clarify.

Thus, we can observe from all the materials analyzed that the higher the absorptance is, the higher the temperature will be; therefore, materials such as black coatings, anodized aluminium samples and solar cells, which have high values of absorptance, will be the ones that end up stabilizing at higher temperatures. Besides the solar cells, that have a strict functional reason to be in the satellite, all of these materials are bound to be used in missions in which the spacecraft will spend a lot of time not receiving sun light, and consequently could end up frozen. For this reason, it is advisable to use these kinds of materials, in order to increase the temperature of the system. The material with the highest absorptance value is a black coating, and, particularly, the Vel-Black.

On the other hand, we can observe that the materials with a lower value of absorptance tend to stabilize at low temperatures. Materials such as Optical Solar Reflectors, some films and tapes, some metals and some vapor-deposited coatings, are the ones that cool down the spacecraft to temperatures that could, in some cases, even end up frosting the satellite if they lack a proper temperature regulation. Missions, not only like the Parker Solar Probe, that was launched directly to the Sun by NASA in order to widen our understanding of the Sun, but also some missions in which the satellite is more exposed to the Sun radiation, would be perfect for using materials that get heated as little as possible possible by the radiation received, such as these. The material with the lowest absorptance value is the Vapor-Deposited Silver.

Table 2
View-factor × area products (m^2). See details in Fortescue et al. (2011)

Nodes	1	2	3	4	5	6	7	8	9	10
1	-	0,068	0,079	0	0	0	0	0,013	0,215	0,058
2	0,068	-	0,089	0	0	0	0	0,018	0,241	0,031
3	0,079	0,089	-	0	0	0	0	0,016	0,246	0,018
4	0	0	0	-	0,089	0,079	0,018	0,016	0,246	0
5	0	0	0	0,089	-	0,068	0,031	0,018	0,241	0
6	0	0	0	0,079	0,068	-	0,058	0,013	0,215	0
7	0	0	0	0,018	0,031	0,058	-	0,0027	0,031	0
8	0,013	0,018	0,016	0,016	0,018	0,013	0,0027	-	0,054	0,0027
9	0,215	0,241	0,246	0,246	0,241	0,215	0,031	0,054	-	0,031
10	0,058	0,031	0,018	0	0	0	0	0,0027	0,031	-

Table 3
Conductance terms (W/K). See details in Fortescue et al. (2011).

Nodes	1	2	3	4	5	6	7	8	9	10
1	-	1,03	0	0	0	0	0	0	0	0,18
2	1,03	-	2,1	0	0	0	0	0	0	0
3	0	2,1	-	2,54	0	0	0	0	1,41	0
4	0	0	2,54	-	2,1	0	0	0	1,41	0
5	0	0	0	2,1	-	1,03	0	0	0	0
6	0	0	0	0	1,03	-	0,18	0	0	0
7	0	0	0	0	0	0,18	-	0,16	0	0
8	0	0	0	0	0	0	0,16	-	0,94	0,16
9	0	0	1,41	1,41	0	0	0	0,94	-	0
10	0,18	0	0	0	0	0	0	0,16	0	–

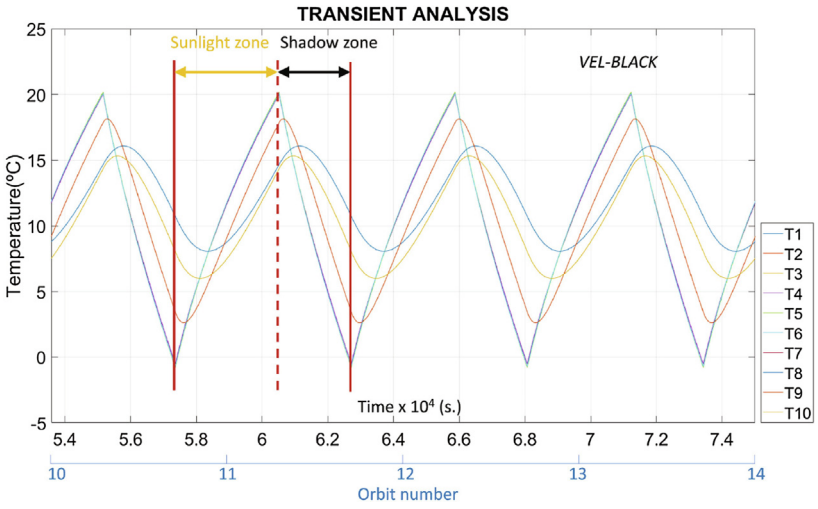

Fig. 4. Nodal thermal evolution in sunlight and shadow zones. Results for Vel-black (Black coatings).

Nevertheless, we find that the emittance does not seem to affect the temperature as much as the absorptance does. Evaluating the graphics, we can assert that the values of emittance dictate in quite a lower scale the value of temperatures.

Finally, we can observe when the values of absorptance and emittance are both very low, with materials like polished silver, vapor-deposited aluminium or vapor-deposited silver, the values get really low, until quite below zero Celsius degrees. In these graphics we can see how the batteries (Node 8) are kept attenuated and in a higher temperature than the rest of the satellite, owing to the fact that they have internal heating.

Therefore, the use of certain materials as coatings would consequently mean that there would be no need of external thermal conditioning. In addition, some other materials,

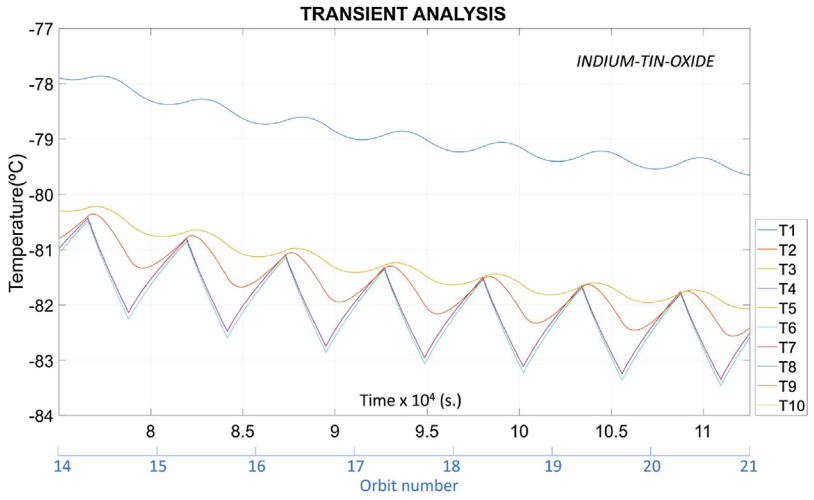

Fig. 5. Nodal thermal evolution in sunlight and shadow zones. Results for Indium-Tin-Oxide (ITO) (Optical Solar Reflector).

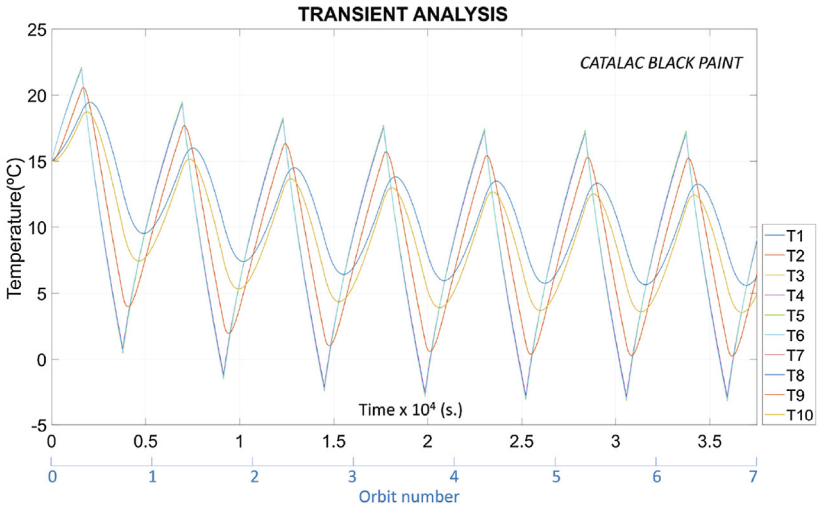

Fig. 6. Nodal thermal evolution in sunlight and shadow zones. Results for Catalac black paint coating (Black Coatings).

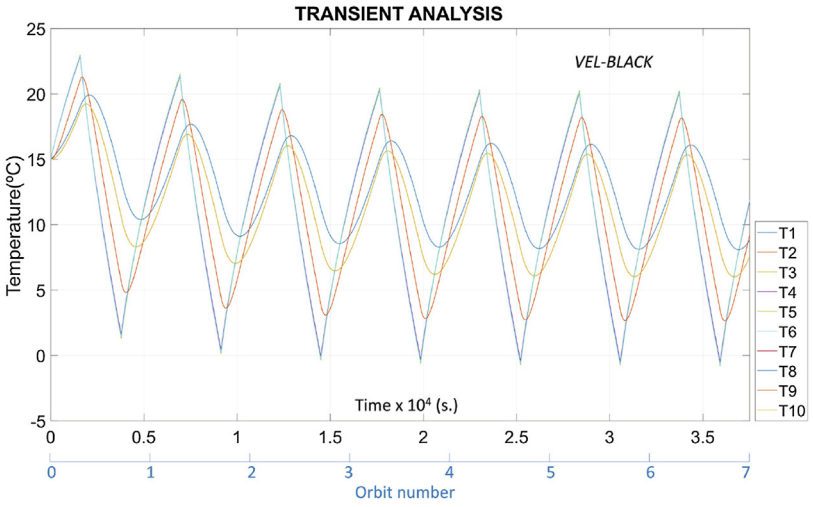

Fig. 7. Nodal thermal evolution in sunlight and shadow zones. Results for Vel-Black paint coating (Black Coatings).

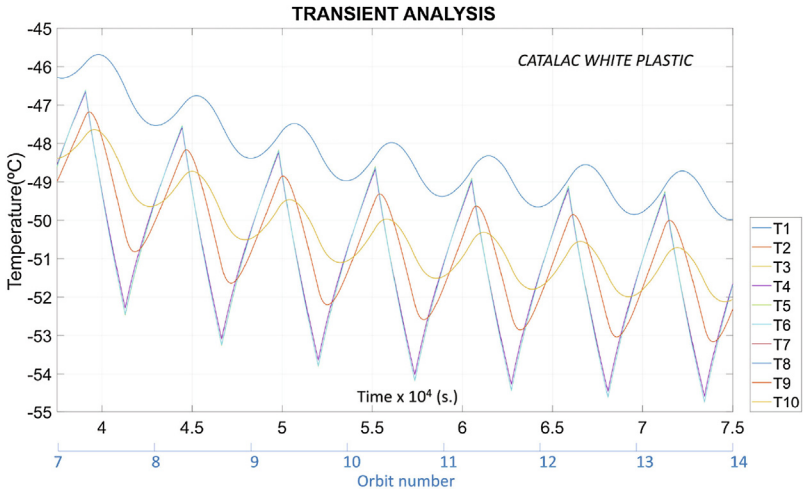

Fig. 8. Nodal thermal evolution in sunlight and shadow zones. Results for Catalac white paint coating (White Coatings).

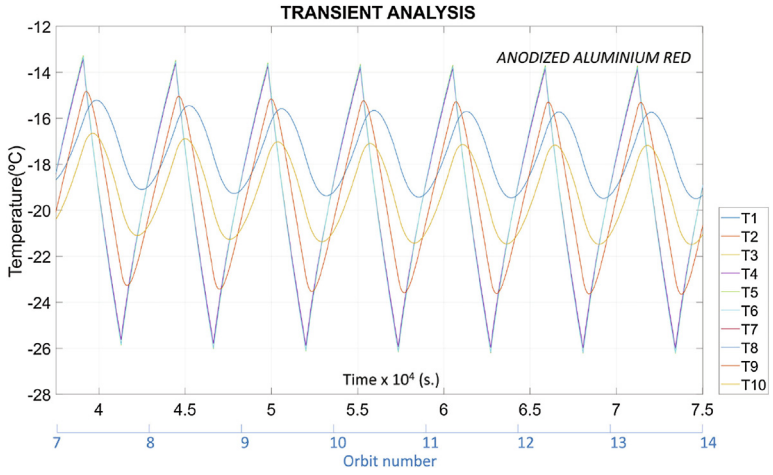

Fig. 9. Nodal thermal evolution in sunlight and shadow zones. Results for Anodized Aluminium Red (Anodizade aluminium)..

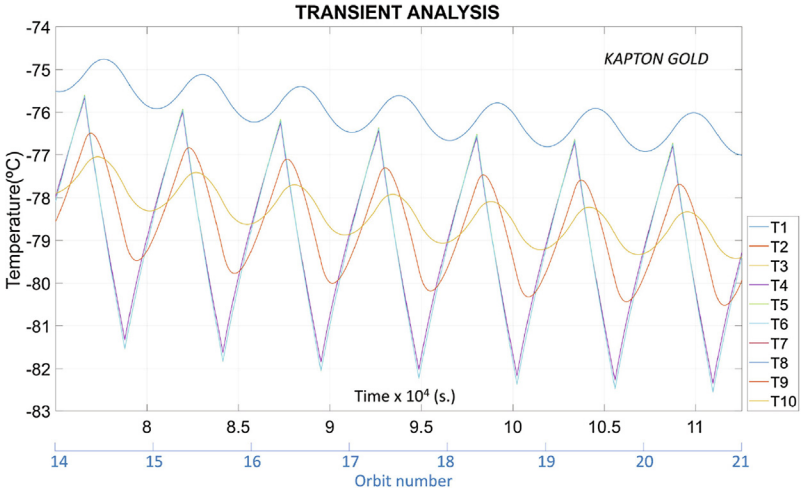

Fig. 10. Nodal thermal evolution in sunlight and shadow zones. Results for Kapton gold (Goldized kapton).

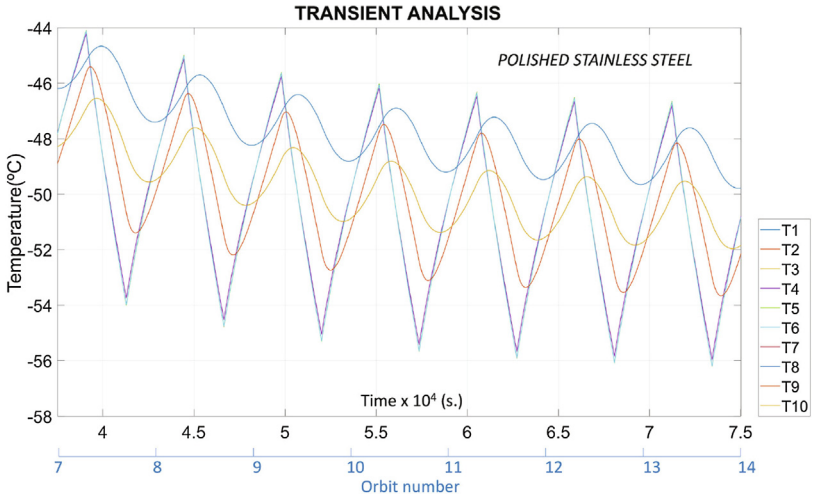

Fig. 11. Nodal thermal evolution in sunlight and shadow zones. Results for Polished Stainless Steel (Metals).

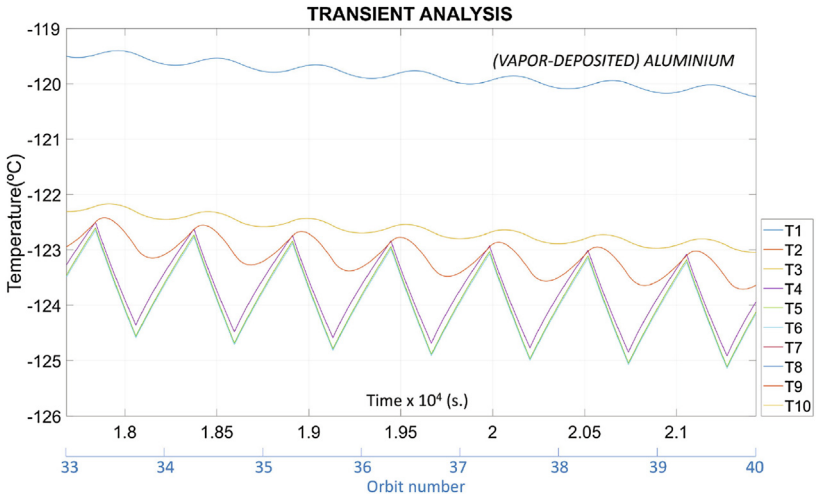

Fig. 12. Nodal thermal evolution in sunlight and shadow zones. Results for Aluminium (Vapor-deposited coating).

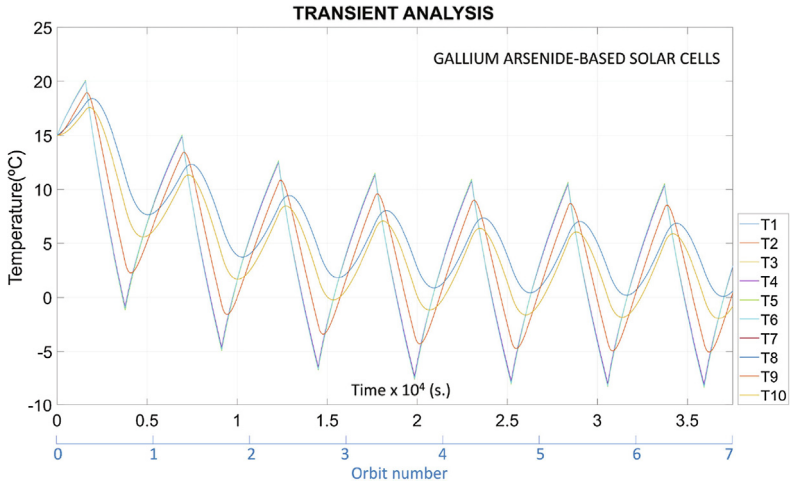

Fig. 13. Nodal thermal evolution in sunlight and shadow zones. Results for Gallium Arsenide-based solar cells (Solar Cells).

such as Gallium Arsenide-based solar cells among others, that accomplish a range of temperatures differing around 10 degrees from the well-functioning range in our benchmark satellite. Thus, the use of certain materials would minimize active thermal conditioning.

7. Conclusions

In this work, the linearized discrete thermal problem for steady-state and transient regime is derived in a backward implicit scheme that lead to an algebraic equations system. This approach has been implemented in Matlab© and described in detail. The backward implicit procedure avoids the numerical problems exhibit by the mostly used forward-explicit scheme.

Thermal control in a satellite is an essential action that must guarantee that all components are going to be submitted in a range of temperature that ensures its correct performance. In certain applications, it is not feasible to use external systems that can keep the satellite within operational temperature limits, therefore, the selection of the parameters that govern the passive thermal control is the underlying question. In this context, choosing the proper coating materials is a key aspect in the design process, as it has been shown in this work.

The implemented code has been applied to a straightforward lumped model of a LEO benchmark satellite obtained from literature. Moreover, the influence on the thermal response of different coating materials has been also studied.

Without prejudice to the general purpose of this work, there are some limitations. Regarding the material properties, the influence of specific heat and conductance is not addressed. In addition, several simplifications have been made in order to obtain the radiation sources (solar, albedo and planetary), according to the simple benchmark satellite problem. Changes in the orbit plane and orientation of the satellite surfaces with respect to the Earth vector are not investigated. All this aspects should be included in a more complex satellite geometry and other orbits.

Declaration of Competing Interest

The authors declare that they have no known competing financial interests or personal relationships that could have appeared to influence the work reported in this paper.

Acknowledgements

The authors acknowledge the Agencia Estatal de Investigación for the financial support received through the project DPI2017-89197-C2-2-R and the Generalitat Valenciana for the Programme PROMETEO 2016/007. The authors declare that they have no conflict of interest.

References

Bonnici, M., Mollicone, P., Fenech, M., Azzopardi, M.A., 2019. Analytical and numerical models for thermal related design of a new picosatellite. Appl. Therm. Eng. 159 (113908), 1–9.

Corpino, S., Caldera, M., Nichele, F., Masoero, M.C., Viola, N., 2015. Thermal design and analysis of a nanostaellite in low earth orbit. Act. Astro. 115 (13), 247–261.

Chapman, A.J., 1987. Fundamentals of Heat Transfer. Macmillian.

Fortescue, P., Swinerd, G., Stark, J., 2011. Spacecraft system engineering, ISBN 978-0-470-75012-4.

Garzón, A., Villanueva, Y.A., 2018. Thermal analysis of satellite Libertad 2: a guide to CubeSat temperature prediction. J. Aerosp. Technol. Manag. 10, e4918. https://doi.org/10.5028/jatm.v10.1011.

Gilmore, D., 2002. Spacecraft thermal control handbook. Volumen I: Fundamental Technologies.

Kauder, L., 2005. Spacecraft thermal control coatings references (NASA/TP-2005-212792).

Knight, R., Pin, O., Thomas, J., 2000. ThermXL: a Thermal Modelling Tool Integrated Within Microsoft Excel, 30th, International Conference on Environmental Systems and 7th European Symposium on Space Environmental Control Systems, Toulouse (France), 9-13.

Zhang, S., Cao, X., Luan, Y., Ma, X., Lin, X., Kong, X., 2011. Preparation and Properties of smart thermal control and radiation protection materials for multi-functional structure of small spacecraft. J. Mater. Sci. Technol. 27 (10), 879–884.